4. EXPERIMENTAL DATA AND RESULTS

4.1 Fluids and Their Properties

The physical and transport properties of the fluids used in the present studies are presented in Table 4.1. Water and Therminol-66 are used as liquid phases, while air and nitrogen are used as gas phases.

The properties of Therminol-66 are taken from the data sheets provided by the supplier and a brief review is given here.

Therminol-66, a Monsanto synthetic heat transfer fluid offers low temperature pumpability with outstanding high temperature performance to 650°F. It is not classified as a fire resistant heat transfer fluid and consequently the use of protective devices may be required to minimize fire risk. To minimize fluid oxidation, it is recommended that systems utilizing Therminol-66 should be blanketed with inert atmoshpere. Therminol-66 is noncorrosive to metals.

Chemically, Therminol-66 is reported by the manufacturers as modified terphenyl having a chemical formula of $C_{18}H_{14}$ with three isomeric forms and a molecular weight of 230.29. Average molecular weight is reported as 240 by the manufacturers. It has a boiling range 643°F or 339°C (10%) - 668°F or 353°C (90%). The fire and flash points are 380° and 350°C respectively. Its specific gravity at 15.5°C is 1.004. Its coefficient of thermal expansion is 0.00047 per °F or 0.00085 per °C. Its calculated heat of vaporization is 114 BTU/lb or 63 Cal/g. The density, specific heat, thermal conductivity and viscosity are given in Table 4.1.

4.2 Slurries and Their Properties

The properties of the slurries are estimated from the individual data of the two phases involved and a suitable combination rule.

The mean densities are calculated from

$$\rho_{sL} = v_s \rho_s + v_L \rho_L \qquad 4.1$$

Table 4.1. Properties of fluids.

Fluid	Temperature °C	Density (kg/m^3)	Viscosity x 10^3 (kg/ms)	Thermal Conductivity (W/mk)	Heat Capacity (kJ/kgK)	Pr (-)
Water	25	997.1	0.890	0.611	4.1809	6.1
	35	994.0	0.719	0.625	4.1777	4.8
	50	988.0	0.544	0.643	4.1791	3.5
	70	977.8	0.400	0.662	4.1920	2.5
	90	965.3	0.311	0.676	4.2107	1.9
Therminol-66	25	1003.4	69.71	0.120	1.6036	1080.6
	35	996.6	37.31	0.119	1.6393	518.0
	50	982.9	13.86	0.118	1.7104	129.3
	100	948.9	3.452	0.114	1.8867	56.9
	150	914.9	1.465	0.111	2.0629	27.3
	200	884.3	0.863	0.107	2.2216	18.2
	250	850.3	0.574	0.102	2.3979	13.7
Air	50	1.185	0.0184	0.0262	1.005	0.702
	35	1.150	0.0189	0.0274	1.005	0.700
	50	1.093	0.0196	0.0285	1.005	0.698
	70	1.029	0.0206	0.0303	1.009	0.694
Nitrogen	25	1.364	0.0184	0.0256	1.029	0.723
	35	1.410	0.0186	0.0267	1.031	0.733
	50	1.478	0.0192	0.0278	1.034	0.688
	100	1.707	0.0208	0.0306	1.044	0.709
	150	1.936	0.0229	0.0338	1.053	0.713
	200	2.165	0.0248	0.0369	1.062	0.714
	250	2.394	0.0266	0.0398	1.076	0.719

where v represents the volume fraction of a particular phase in the mixture, and s and L refer to solid and liquid phases respectively.

The heat capacity of the slurry is given by

$$C_{p,sL} = w_S C_{ps} + w_L C_{pL} \qquad 4.2$$

where w represents the weight fraction of solids in the slurry. For estimating the slurry thermal conductivities, Tareef [51] proposed the relation:

$$k_{sL} = k_L \frac{2k_L + k_S - 2V_S (k_L - k_S)}{2k_L + k_S - v_S (k_L - k_S)} \qquad 4.3$$

The viscosities of the slurries are obtained from Vand's equation [52]:

$$\mu_{sL} = \mu_L \exp\left(\frac{2.5\, v_S}{1 - 39v_S/64}\right) \qquad 4.4$$

4.3 Gas Holdup Data for Small Column

The experimental gas holdup studies (both total and local) are carried out in the 0.108 m diameter bubble column either in continuous or batch mode with respect to liquid or slurry, and in continuous mode with respect to gas phase. The gas and liquid flows are cocurrent and the experiments are carried out at about atmospheric pressure. The bubble column is equipped with internals of different types and the liquids (slurries) used covered a wide range of viscosity, density and surface tension. The ranges of properties of fluids used in the present study are given in Table 4.1.

4.3.1 Operating Mode and a Typical Procedure

To determine the local gas holdup in the column, pressure profile along the column height is established first by measuring pressure at ten locations. The

pressure measurement and control systems are shown in Figs. 3.1 and 3.3. At a given location the hydrostatic head is balanced out by suitably adjusting the purge-rotameter flow rate and only a minimum amount of gas is allowed to flow through the pressure ports. The local gas holdup for set values of experimental conditions is given by the following equation where the manometer readings are converted to absolute pressure by the simple hydrostatic head technique

$$\epsilon'_g (U_g , h) = 1 - \Delta P \, [H \, (\rho_m - \rho_g)]^{-1} \qquad 4.5$$

here h represents the height above the gas distributor plate; H the height of the section; U_g , the superficial gas velocity; ΔP, the pressure drop across the sections; ρ_m the density of manometer liquid; and ρ_g , the density of the gas.

The average gas holdup for a set of liquid and gas flow rates is computed from known values of initial slumped height (H_s) of liquid (or slurry) and the expanded height of the dispersion (H_e). For continuous operation, the dispersion height (H_e) is fixed at 1.72 m, and the overflow is collected in a reservoir and eventually recirculated. For semi-batch operation, the gas holdup is obtained for both increasing and decreasing modes of gas velocity. For a typical run the dispersion height is noted after allowing the system to run for a period of time at the steady-state condition usually 10-15 min. , and the gas flow is cut off to establish the bubble-free settled height (H_s) of liquid (or slurry). While noting the settled height (H_s), care is taken to prevent liquid from leaking through the gas distributor plate by appropriately pressurizing the gas calming section. From the measured values of H_e and H_s, the total gas holdup is calculated from the following relation:

$$\epsilon_g(U_g) = \frac{H_e(U_g) - H_s(U_g)}{H_e(U_g)} \qquad 4.6$$

4.3.2 Air-Water system

4.3.2.a Effect of H_S

Air holdup data are measured in the 0.108 m bubble column as a function of air velocity for slumped heights of liquid in the range 0.80-0.99 m. It is observed from the results in Figs. 4.1A and 4.2A that air holdup depends both on the initial liquid column height and the manner in which the air velocity is varied. The air holdup dependence is predominantly on the degree of foaming. The local air holdup data obtained under similar conditions are presented in Figs. 4.1B and 4.2B. These suggest that the local holdup values are also influenced by the manner in which the air velocity is varied.

4.3.2.b Effect of V_L

Air holdup values are measured for continuous mode of operation for air-water system with both air and water in cocurrent upward flow. In these runs the expanded height of the dispersion is kept constant at 1.702 m, and the corresponding H_S value at a given air velocity is obtained my simultaneously stopping the air and water flows. The results are presented in Fig. 4.3, and it can be seen that both liquid velocity and the manner in which the air velocity is changed has little influence on air holdup for $U_g < 0.07$ m/s. At higher air velocities, $U_g > 0.07$ m/s, the air holdup for both increasing and decreasing U_g is negligibly influenced by liquid velocity and the hysteresis effect present at zero liquid flow velocity is also absent.

4.3.2.c Effect of Internals

The bubble size is influenced by the presence of tube internals in the column. A comparison of data from Figs. 4.1 and 4.2 revealed that the holdup is significantly larger for tube internals in comparison to unbaffled column for otherwise under identical operating conditions. The dependence of ϵ_g on H_S (Fig. 4.2A) is viewed as due to the limitation of bubble breakage by baffles at greater values of H_S.

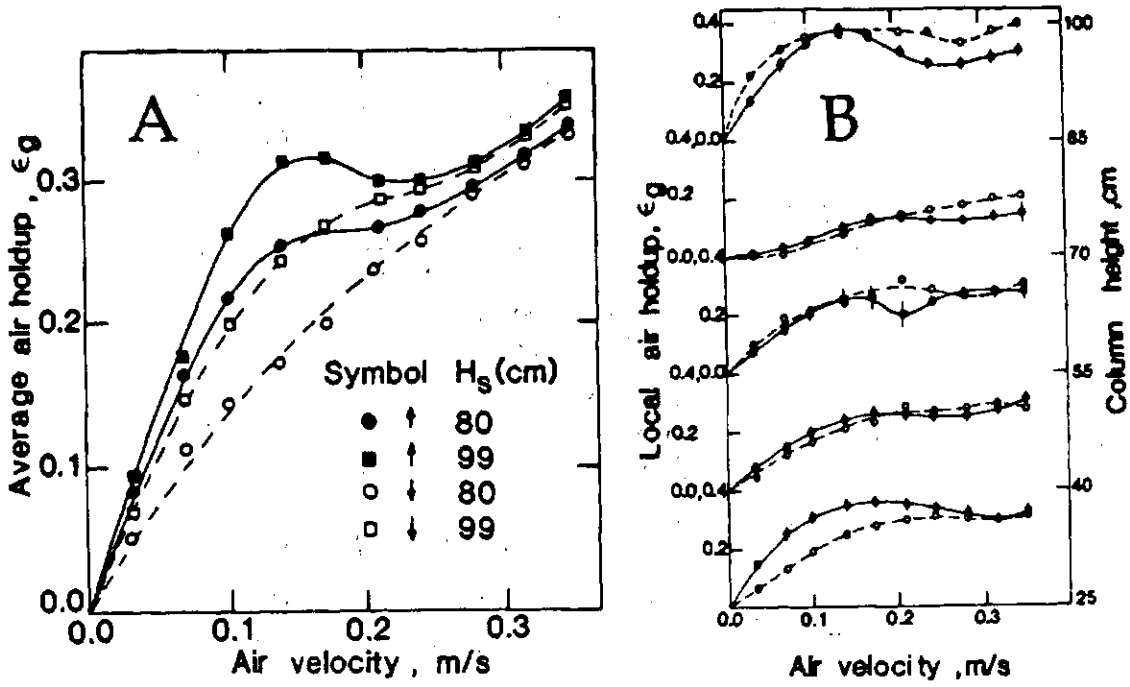

Fig. 4.1. Variation of gas holdup with increasing and decreasing air velocity for different slumped water column height: (A) average, (B) local.

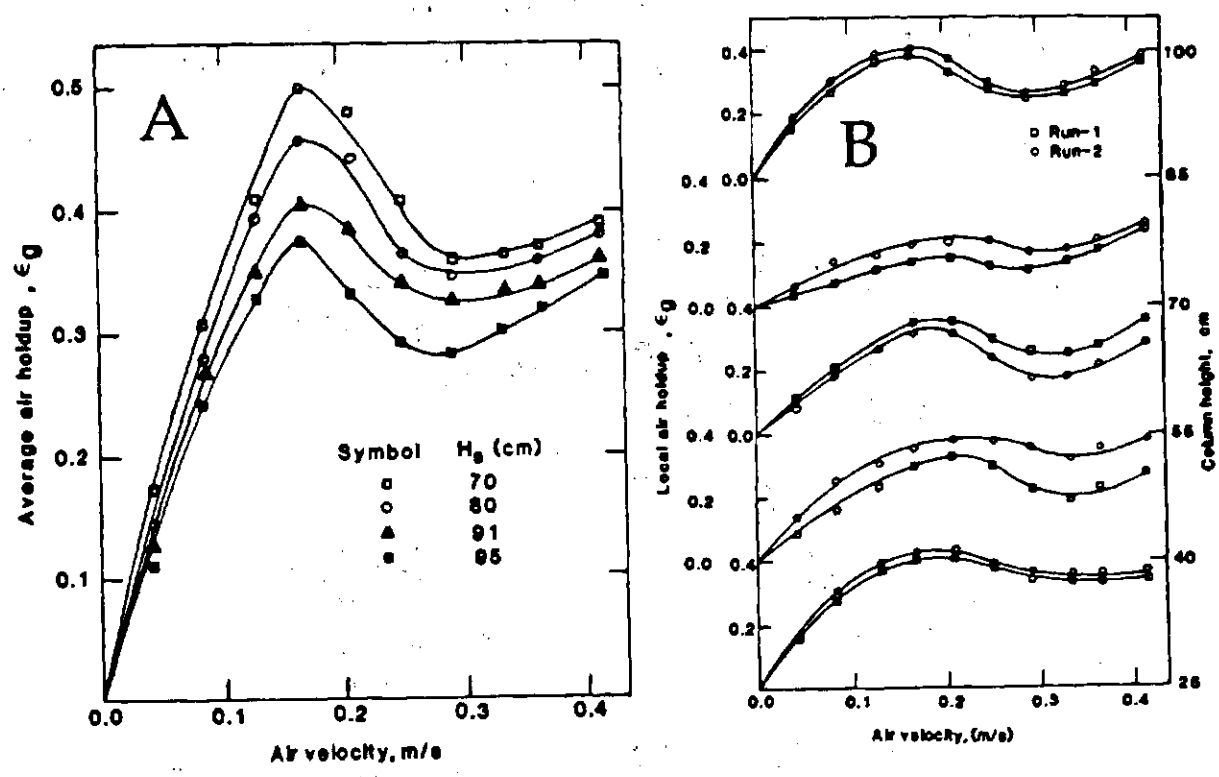

Fig. 4.2. Variation of air holdup with air velocity and slumped water column height: (A) average, (B) local.

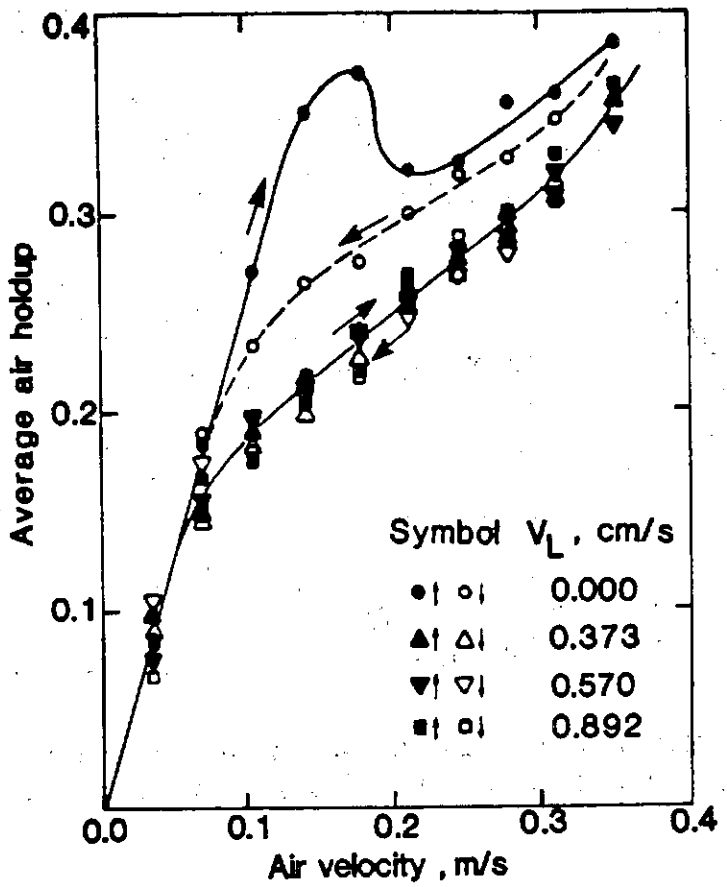

Fig. 4.3. Variation of average air holdup with air and liquid velocities.

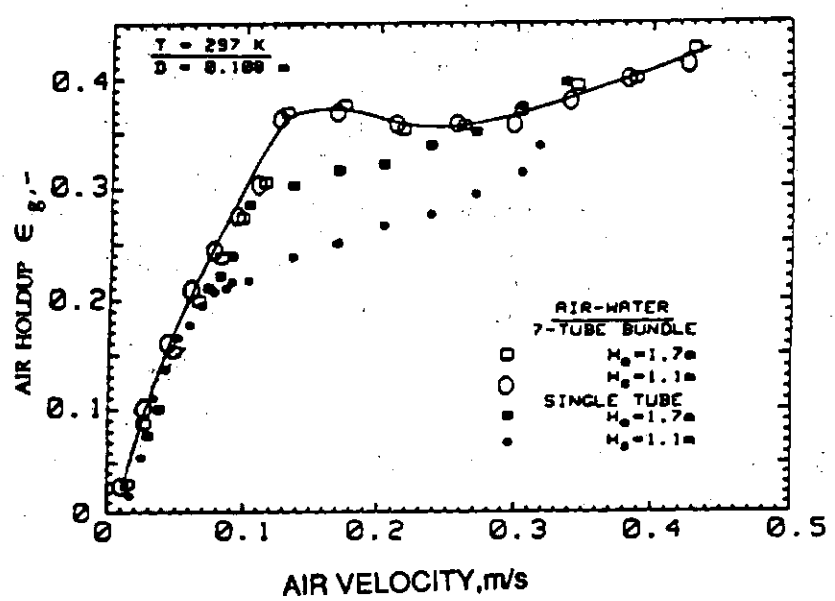

Fig. 4.4. Dependence of average air holdup on air velocity and tube bundle size.

A similar study of the influence of internals on air holdup is done with a seven-tube bundle for decreasing air velocity. In the first mode, the initial unaerated height of the water column is kept constant at 1.1m. In the second mode the expansion height of the dispersion is maintained constant at 1.7m and the corresponding H_s value is measured by cutting off the air supply.

In Fig. 4.4, are shown for comparison the air holdup data taken for the two modes when only a single tube instead of the tube bundle is present in the column. For both the modes, the values for the single tube are smaller than the corresponding values for the tube bundle. The differences are particularly appreciable in the region of air velocities from 0.1 to 0.3 m/s, where the bubble coalescence and circulating cells play a significant role. The seven-tube bundle configuration prevents the formation of larger coalesced bubbles and hence the air holdup is larger. The smaller holdup values for the single tube and first mode of operation is due to the differences in the pattern of formation of circulating liquid cells.

The data of Fig. 4.4 clearly demonstrate that the nature of internals plays only an insignificant role in the free bubbling and slugging regimes. On the other hand in the coalescing bubble flow regime where circulating liquid plays an important role, the nature of baffles is very important and it significantly influences the value of gas holdup at a given gas velocity.

Three independent sets of the gas holdup data obtained for air-water system in the small column equipped with a 19mm heat transfer probe are given in Table 4.2. Similar data obtained with a seven-tube internal are presented in Table 4.3.

4.3.3 Nitrogen - Therminol system

The experimental total gas holdup studies are conducted in the 0.108 m bubble column equipped with one of the either three single tubes or a seven-tube bundle in batch mode. The system studied involves a highly viscous fluid,

Table 4.2. Experimental air holdup values for air-water system at 309K. Column diameter: 0.108 m, Internal: 19mm single tube.

SET - 1		SET - 2		SET - 3	
U_g (m/s)	ϵ_g (-)	U_g (m/s)	ϵ_g (-)	U_g (m/s)	ϵ_g (-)
0.0086	0.039	0.0130	0.013	0.0086	0.003
0.0130	0.057	0.0215	0.060	0.0170	0.045
0.0170	0.070	0.0301	0.095	0.0258	0.088
0.0215	0.076	0.0344	0.107	0.0344	0.102
0.0258	0.083	0.0387	0.124	0.0430	0.132
0.0301	0.098	0.0430	0.133	0.0473	0.125
0.0344	0.107	0.0473	0.143	0.0516	0.155
0.0388	0.116	0.0560	0.164	0.0560	0.164
0.0430	0.117	0.0645	0.182	0.0602	0.172
0.0473	0.126	0.0688	0.191	0.0645	0.173
0.0516	0.127	0.0730	0.197	0.0688	0.186
0.0560	0.132	0.0774	0.208	0.0730	0.189
0.0602	0.133	0.0817	0.212	0.0817	0.213
0.0645	0.136	0.0860	0.224	0.0860	0.205
0.0688	0.136	0.0832	0.251	0.116	0.248
0.0730	0.148	0.099	0.280	0.148	0.246
0.0774	0.149	0.115	0.298	0.181	0.252
0.0917	0.153	0.132	0.307	0.214	0.262
0.0860	0.154	0.148	0.302	0.247	0.315
		0.181	0.327	0.281	0.325
		0.214	0.345	0.313	0.326
		0.247	0.352	0.333	0.351
		0.281	0.367		
		0.313	0.383		
		0.333	0.386		

Table 4.3. Experimental air holdup values for air-water system at 297K. Column diameter: 0.108m, Internal: Seven-tube bundle.

Air velocity (m/s)	Air holdup	
	Set 1	Set 2
0.022	0.074	0.077
0.044	0.147	0.150
0.066	0.201	0.206
0.088	0.238	0.245
0.110	0.267	0.267
0.128	0.304	0.301
0.192	0.338	0.310
0.256	0.350	0.331
0.319	0.376	0.360
0.362	0.378	-
0.384	-	0.380
0.426	0.404	-

Therminol-66, and the experiments are conducted at about ambient conditions of temperature and pressure.

4.3.3.a Effect of H_S

Six different sets of nitrogen holdup, five for decreasing and one for increasing gas velocities, at different slumped Therminol column heights (H_S) are taken with the results reported in Fig. 4.5. All the five sets taken with decreasing gas velocity are in good agreement with each other. The gas holdup data for increasing nitrogen velocity appear to have a tendency of greater holdup values. This trend is more obvious at higher U_g. No foaming is observed and the nitrogen holdup is computed from the knowledge of the liquid column height for a finite and zero value of the gas velocity.

A few remarks about the bubbling and bubble coalescence phenomenon observed in the column are in order. At low nitrogen velocities ($\leq$ 3 cm/s) bubbles are formed at the distributor plate from varying region of the plate having an initial size of 4-5 mm diameter. These bubbles in discrete identity rise through the liquid column (> 9 cm/s) to a size as big as 15 mm diameter. No liquid circulation is observed in the column. Bubble coalescence is predominant in the velocity range $3 \leq U_g \leq 8$ cm/s and bubbles as large as 40 mm are observed at about 8 cm/s. With further increase in gas velocity the bubble size increased to 70 mm at about U_g = 20 cm/s.

4.3.3.b Effect of Internals

The effect of internals on gas holdup is presented in Fig. 4.6. It is observed that the internals has negligible influence on bubble coalescence behavior and hence on the total gas holdup.

Smoothed values of nitrogen holdup for the nitrogen-Therminol system for the single tubes are presented in Table 4.4 and for a seven-tube bundle in

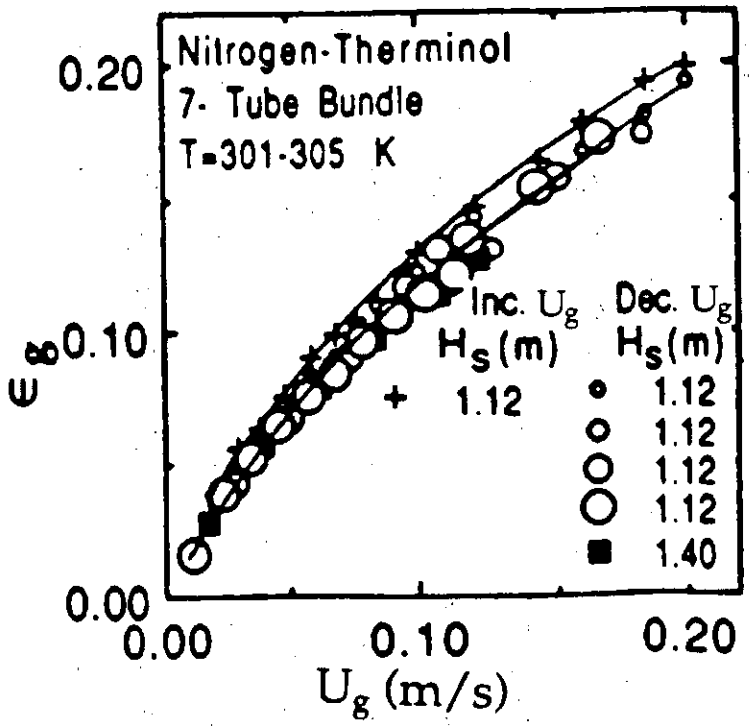

Fig. 4.5. Variation of average air holdup for increasing and decreasing nitrogen velocity and different slumped liquid column height..

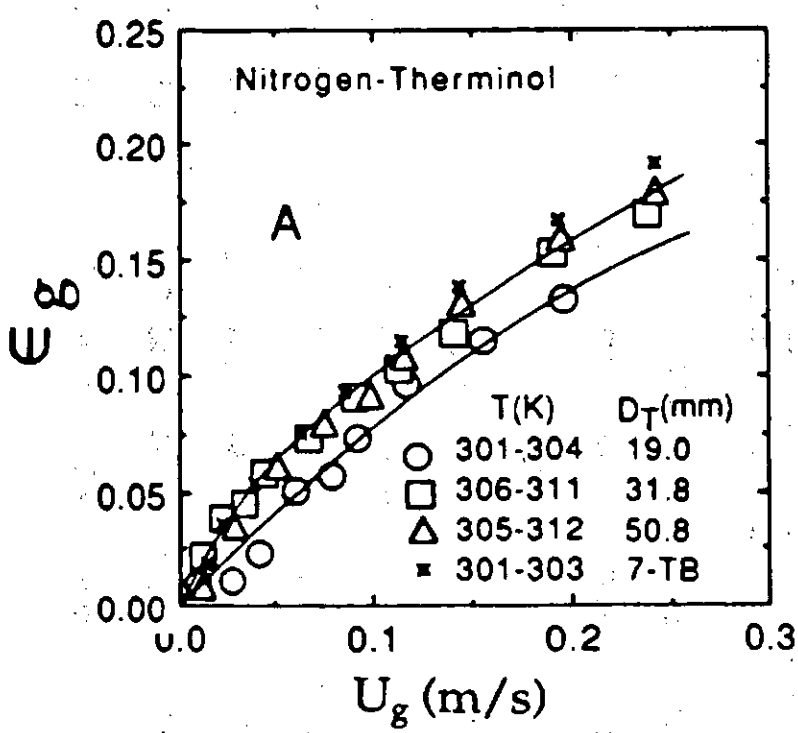

Fig. 4.6. Dependence of nitrogen holdup on decreasing nitrogen velocity for heat transfer probes of different diameters and seven-tube bundle.

Table 4.4. Smoothed nitrogen holdup values for nitrogen-Therminol-magnetite system at 306K. Column diameter: 0.108 m, Internals: 19 mm, 31.8 mm, and 50.8 mm single tubes, Solids conc. : 0, 15, 30 and 50 wt %.

U_g	0%	15%	30%	50%	0%	15%	30%	50%	0%	15%	30%	50%
(m/s)	19.0 mm				31.8 mm				50.8 mm			
0.025	0.021	0.022	0.023	0.025	0.041	0.040	0.022	0.020	0.025	0.025	0.026	0.027
0.050	0.054	0.055	0.056	0.057	0.067	0.065	0.045	0.038	0.051	0.052	0.053	0.054
0.075	0.083	0.086	0.087	0.090	0.089	0.088	0.065	0.052	0.076	0.076	0.077	0.080
0.100	0.104	0.106	0.108	0.110	0.105	0.104	0.082	0.068	0.096	0.097	0.099	0.106
0.125	0.119	0.121	0.123	0.125	0.122	0.141	0.095	0.080	0.118	0.119	0.121	0.124
0.150	0.130	0.134	0.136	0.140	0.140	0.153	0.112	0.090	0.136	0.138	0.140	0.145
0.175	0.138	0.142	0.146	0.149	0.150	0.155	0.124	0.098	0.150	0.152	0.154	0.159
0.200	0.143	0.145	0.150	0.155	0.162	0.165	0.132	0.102	0.162	0.164	0.167	0.172

Table 4.5.

4.3.4 Air-Water-Red Iron Oxide System

The air holdup data is measured for the three-phase system as a function of air velocity and slurry concentration for two different size powders. The holdup values are measured for decreasing air velocity and 19 mm single-tube internal. The average values of solid and liquid holdup are also determined and are shown plotted in Fig. 4.7. These values are computed using the following relationships:

$$\epsilon_g = \frac{H_e - H_{SL}}{H_e} \qquad 4.7$$

$$\epsilon_g = \frac{H_S - H_L}{H_e}$$

$$= \frac{(1 - \epsilon_g)(H_S - H_L)}{H_S} \qquad 4.8$$

and

$$\epsilon_L = \frac{H_L}{H_e}$$

$$= 1 - \epsilon_g - \epsilon_s \qquad 4.9$$

It is observed that air holdup decreases with increasing C_s, signifying the coalescence promoting nature of the slurries, with increasing concentration. These results are consequence of the increase in apparent viscosity of the slurry due to the presence of solids.

Foaming is observed in the two-phase (air-water) system, but it disappeared when iron oxide powder was added. This is shown in Fig. 4.7, where ϵ_g is a monotonically increasing function of increasing air velocity for all values of C_s except zero. The air holdup data is presented in Table 4.6.

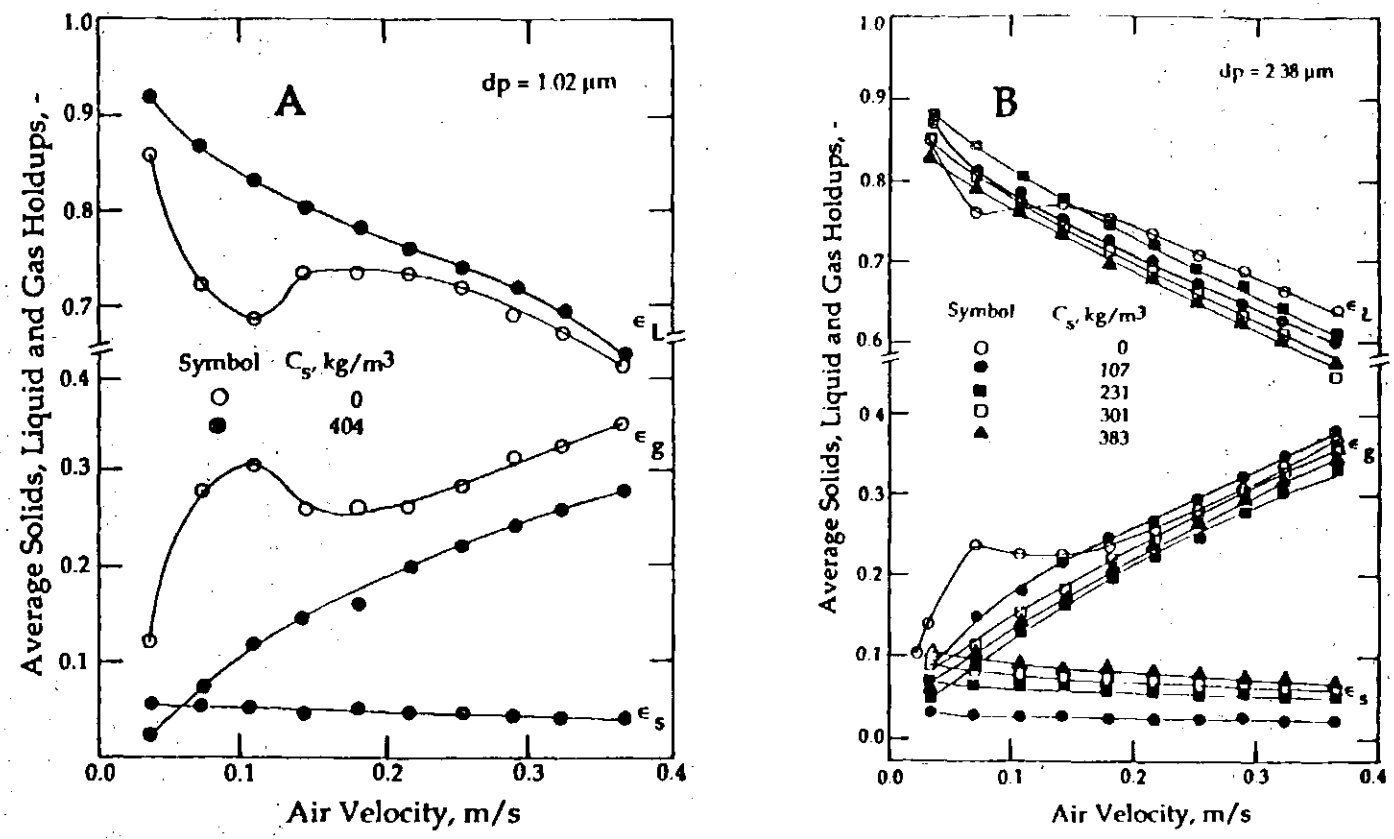

Fig. 4.7. Variation of average red iron oxide, water and air holdups as a function of decreasing air velocity in the column at 295K with a coaxial heat transfer probe (A) d_p = 1.02 μm; and (B) d_p = 2.38 μm.

Table 4.5. Smoothed nitrogen holdup values over a concentration range for nitrogen-Therminol-magnetite system at 306K. Column diameter: 0.108 m, Internal: Seven-tube bundle, particle diameters: 27.7 and 36.6 μm.

Nitrogen Velocity	Nitrogen holdup	Nitrogen Holdup 27.7 μm		36.6 μm	
(m/s)	(-)	0-15%	30-47%	0-15%	30-50%
0.02	0.031	0.030	0.020	0.036	0.028
0.04	0.075	0.060	0.044	0.059	0.048
0.06	0.097	0.080	0.063	0.081	0.065
0.08	0.113	0.105	0.080	0.100	0.082
0.10	0.130	0.125	0.098	0.119	0.099
0.12	0.145	0.139	0.114	0.134	0.115
0.14	0.160	0.155	0.130	0.149	0.128
0.16	0.175	0.169	0.144	0.162	0.138
0.18	0.187	0.180	0.157	0.175	0.148
0.20	—	0.190	0.167	0.188	0.156
0.22	—	0.200	0.177	0.198	0.165
0.24	—	0.210	0.185	0.210	0.170

Table 4.6. Experimental air holdup values for air-water-red iron oxide and air-water-magnetite systems at 295K. Column dimeter: 0.108m, Internal: 19mm single tube.

U_g	Air holdup						
	Iron oxide (1.02 μm)		Iron oxide (2.38 μm)			Magnetite (43.6 μm)	
(m/s)	C_s(kg / m^3)= 108	= 404	=107	=231	= 383	= 167	= 258
0.036	0.114	0.023	0.033	0.051	0.073	0.093	0.082
0.108	0.231	0.120	0.183	0.130	0.140	0.300	0.204
0.145	0.249	0.147	0.221	0.165	0.195	0.370	0.324
0.181	0.263	0.162	0.242	0.195	0.208	0.370	0.319
0.217	0.269	0.201	0.266	0.219	0.244	0.356	0.329
0.253	0.293	0.217	0.307	0.261	0.255	0.350	0.339
0.289	0.324	0.239	0.326	0.277	0.306	0.354	0.338
0.325	0.358	0.263	0.351	0.309	0.327	0.372	0.367
0.362	0.379	0.310	0.377	0.344	0.351	0.390	0.381

4.3.5 Air-Water-Glass bead System

The air holdup data for the air-water-glass bead system with a 19 mm single-tube internal are shown plotted in Fig. 4.8 as a function of U_g , d_p and C_s. It is clear that the particle size in the slurry is not influencing the air holdup and its values are smaller than the corresponding air-water system values over the entire velocity range. This result is to be understood from the fact that bubble coalescence is predominant in the presence of solid particles due to the increase in apparent viscosity.

Similar air holdup data are measured with a seven-tube bundle and as functions of U_g, d_p and C_s. The air holdup results are presented in Fig. 4.9 and these indicate that C_s has little influence for the range less than 10 wt.% but results in decreased holdup for values greater than 10 wt.%.

Expermental air holdup data corresponding to Fig. 4.8 are presented in Table 4.7. Similarly, air holdup data obtained under identical conditions but using two types of internals are presented in Table 4.8. The data for the three-phase system smoothed over particle size range are also presented in this table.

4.3.6 Air-Water-Magnetite System

The air holdup is measured for air-water-magnetite powders as a function of air velocity and solids concentration. The data sets are graphed in Figs. 4.10 A-F. In Table 4.9 are given the values of solids concentration, weight fraction percentage and the range of air velocity used in experiments with each powder. One to three concentrations of the magnetite powder in the slurry are employed. In each case the data for the two-phase (air-water) system, taken in the same fashion, are also shown (curve 4) for comparison. The following general conclusions from these measurements are evident.

(a) The air holdup at a given velocity in the two-phase system does not differ appreciably from that in the three-phase system. The differences between the two sets of values tend to increase with the concentration of solids in the slurry, and it appears that such differences may increase with the size of the solid

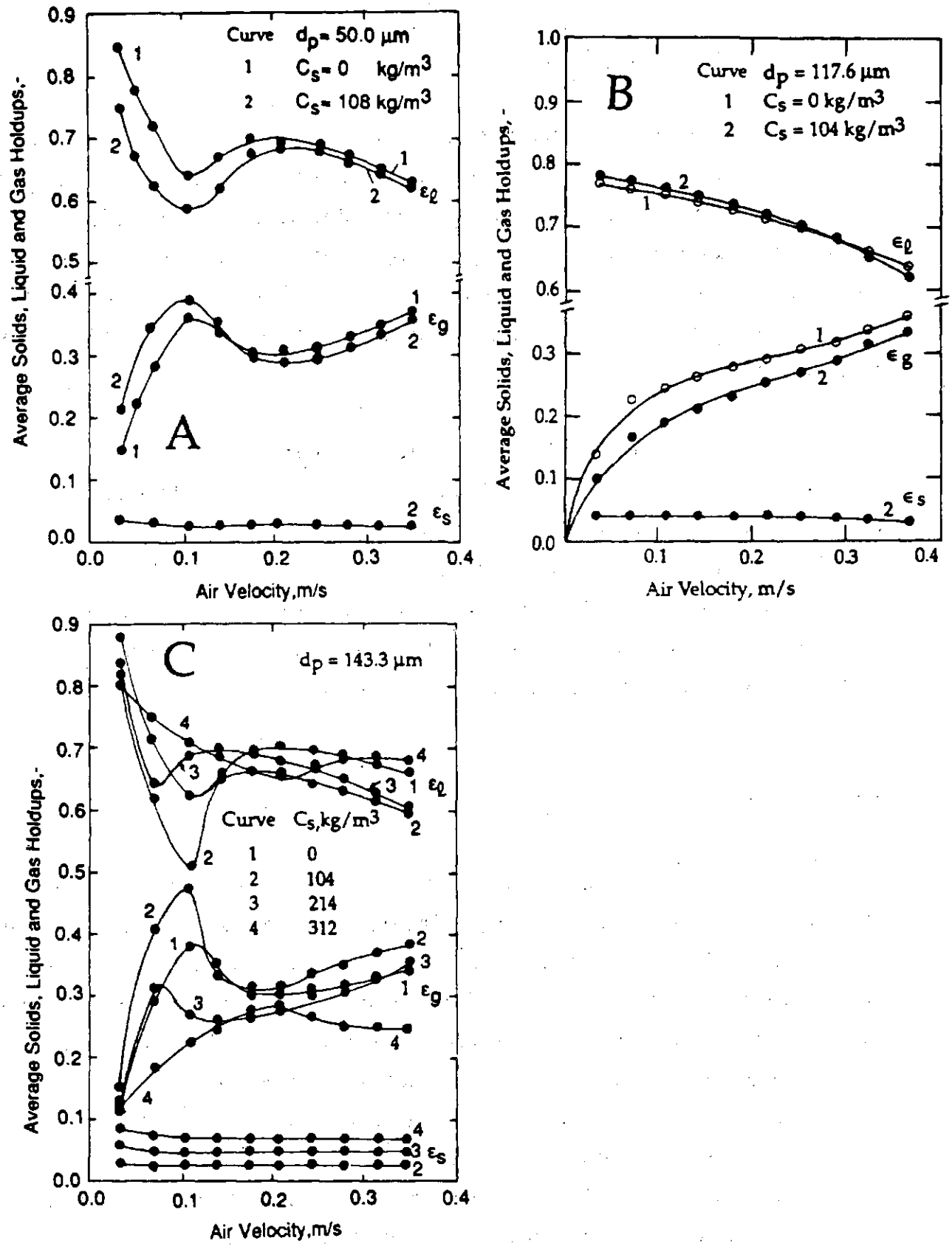

Fig. 4.8. Variation of average solids, liquid and gas holdup as a function of decreasing air velicty and solids concentration for glass beads of (A) 50.0 μm, (B) 117.6 μm, and (C) 143.3 μm.

Table 4.7. Experimental air holdup values for air-water-glass bead system at 309K. Column diameter: 0.108m, Internal: 19mm single probe.

U_g (m/s)	air-water	50µm	117.6µm	143.3µm		
		108 kg/m^3	104 kg/m^3	104 kg/m^3	214 kg/m^3	312 kg/m^3
0.362	0.371	0.353	0.341	0.383	0.355	0.244
0.325	0.349	0.333	0.316	0.368	0.327	0.253
0.289	0.327	0.312	0.284	0.329	0.305	0.247
0.253	0.309	0.292	0.269	0.336	0.297	0.266
0.217	0.312	0.288	0.246	0.317	0.281	0.282
0.181	0.301	0298	0.231	0.312	0.263	0.267
0.145	0.334	0.354	0.210	0.328	0.256	0.242
0.108	0.360	0.390	0.191	0.475	0.268	0.219
0.072	0.279	0.355	0.186	0.405	0.313	0.183
0.036	0.148	0.215	0.177	0.156	0.108	0.116

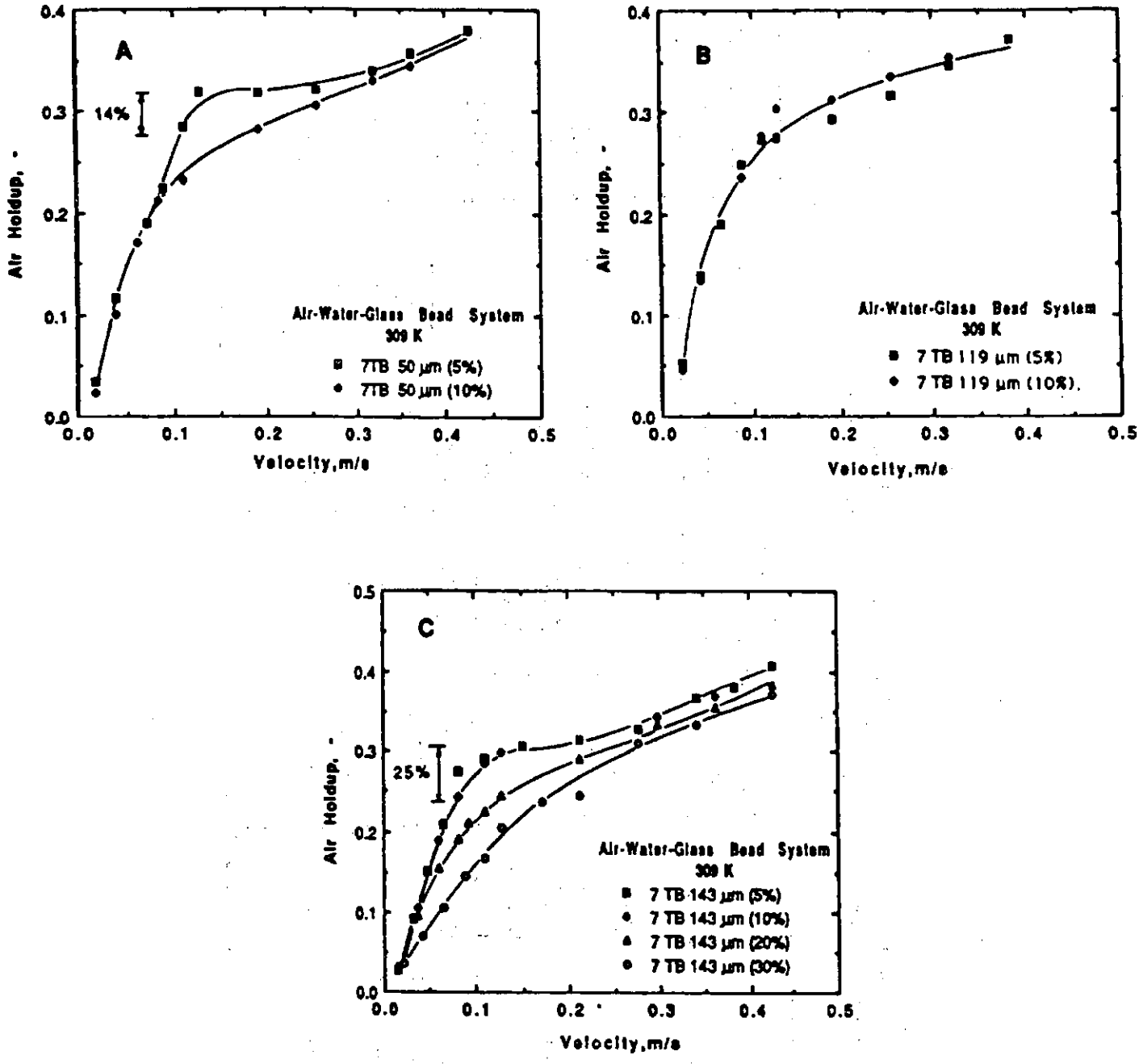

Fig. 4.9. The effect of slurry concentration on air holdup for the 7TB arrangement: (A) 50 μm, (B) 119 μm, and (C) 143 μm.

Table 4.8. Smoothed air holdup values for air-water-glass bead system at 309K. Column diameter: 0.108 m, Internals: 19 mm Single tube and seven-tube bundle, Particle diameters: 50, 119 and 143 μm.

Air Velocity (m/s)	Air-Water		Air-Water-Glass Beads (10Wt%)						Air-Water-Glass Beads (10Wt%) (50,119,143 μm)	
			50 μm		119 μm		143 μm			
	ϵ_{1T}	ϵ_{7T}	ϵ_{1T}	ϵ_{7T}	ϵ_{1T}	ϵ_{7T}	ϵ_{1T}	ϵ_{7T}	ϵ_{1T}	ϵ_{7T}
0.02	0.06	0.06	0.03	0.054	0.03	0.032	0.018	0.03	0.030	0.042
0.04	0.125	0.145	0.09	0.134	0.075	0.128	0.073	0.140	0.085	0.120
0.08	0.180	0.233	0.150	0.205	0.144	0.232	0.123	0.240	0.147	0.220
0.12	0.215	0.285	0.183	0.243	0.195	0.288	0.175	0.291	0.187	0.278
0.16	0.242	0.316	0.211	0.270	0.223	0.310	0.205	0.310	0.215	0.300
0.20	0.262	0.338	0.230	0.292	0.244	0.322	0.232	0.317	0.237	0.310
0.24	0.275	0.352	0.248	0.308	0.260	0.333	0.254	0.323	0.255	0.318
0.28	0.290	0.365	0.262	0.322	0.273	0.342	0.273	0.335	0.270	0.328
0.32	0.298	0.373	0.273	0.333	0.282	0.350	0.290	0.348	0.282	0.340
0.36	0.303	0.378	0.284	0.342	0.290	0.357	0.303	0.363	0.291	0.355
0.40	0.310	0.381	0.293	0.350	0.296	0.362	0.320	0.382	0.300	0.380

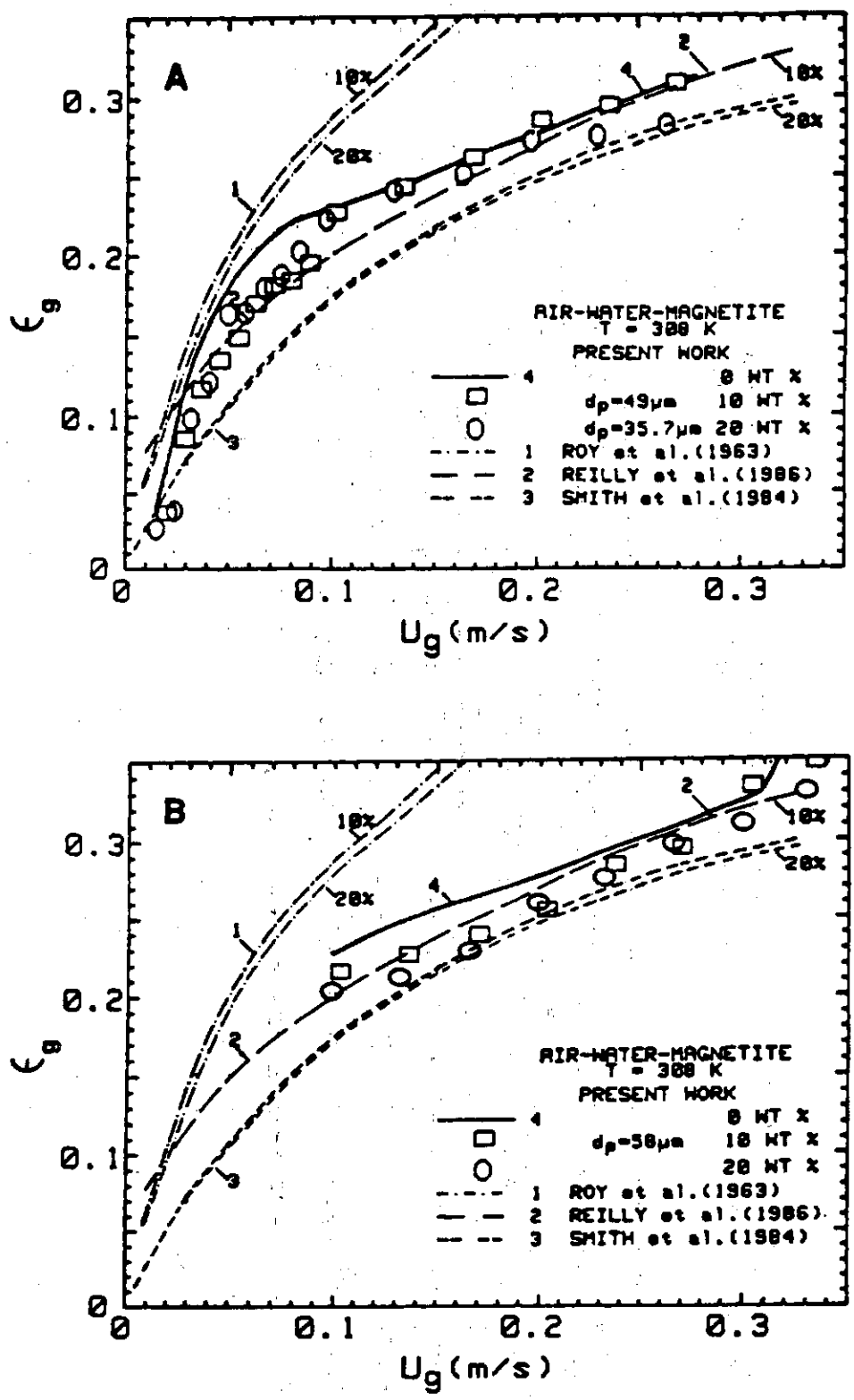

Fig. 4.10. Dependence of ϵ_g on U_g and w_s for magnetite particles of different sizes. The data are also compared with the predictions of three models.

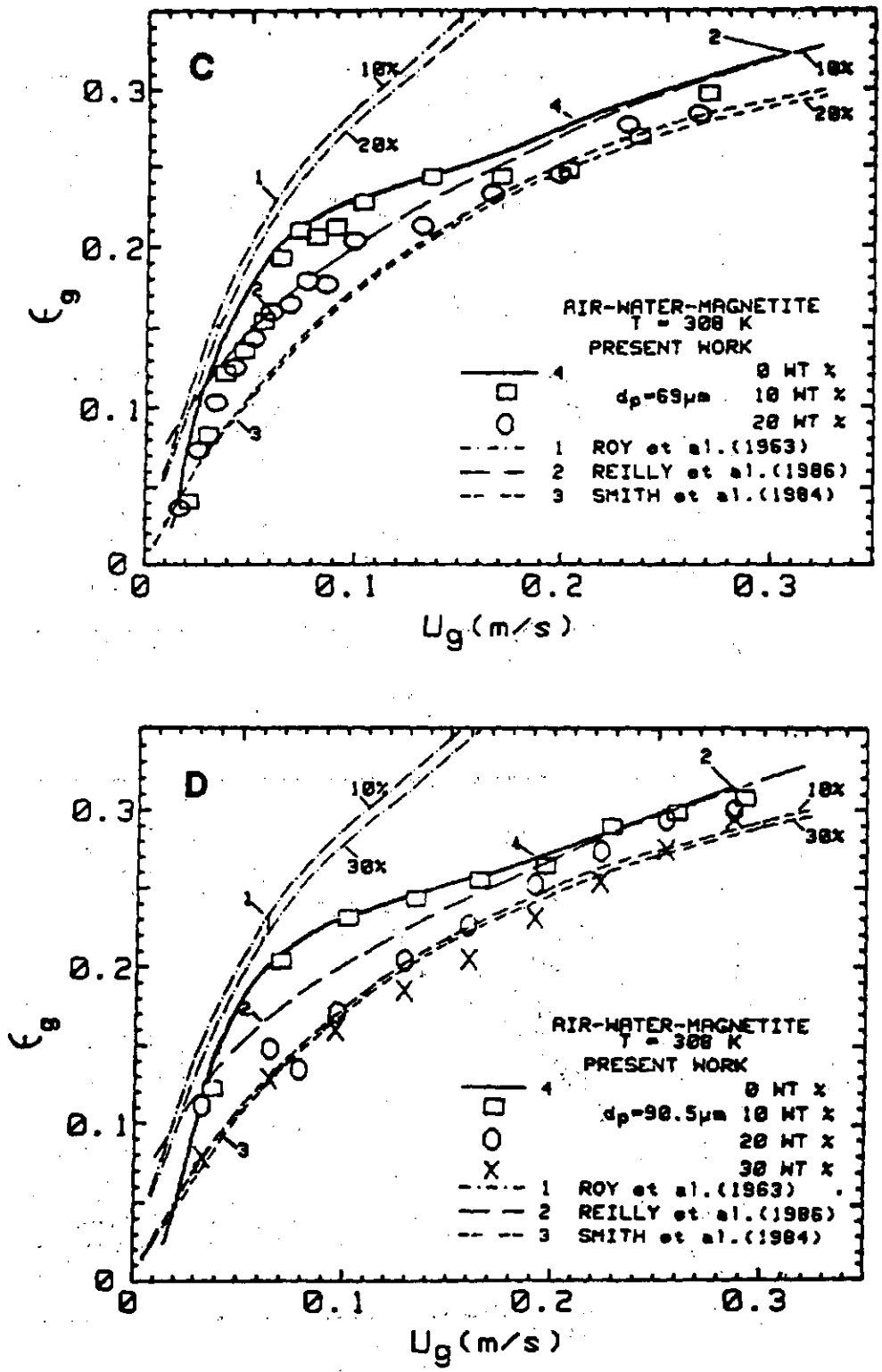

Fig. 4.10. Dependence of ϵ_g on U_g and w_s for magnetite particles of different sizes. The data are also compared with the predictions of three models. Fig.

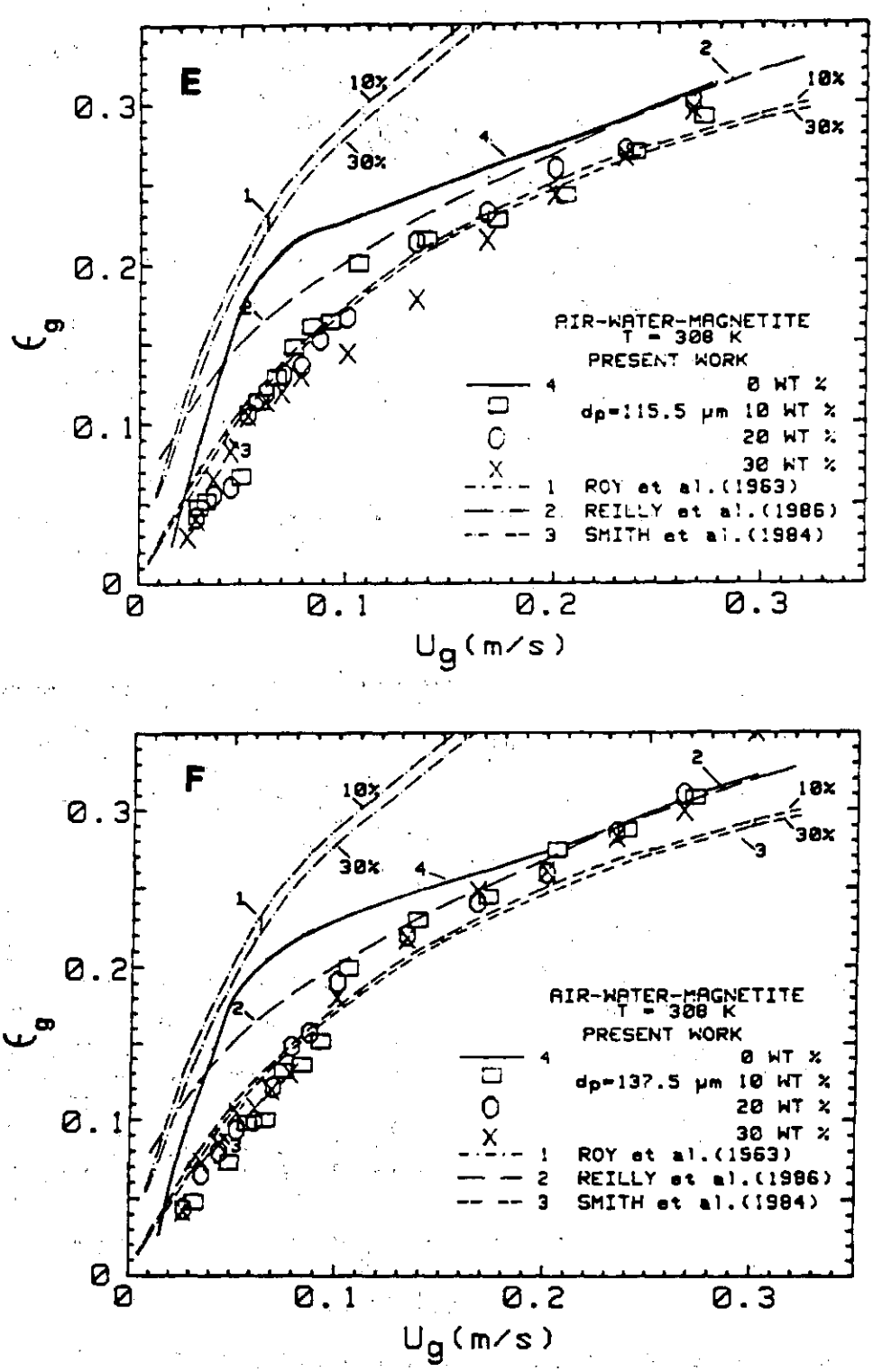

Fig. 4.10. Dependence of ϵ_g on U_g and w_s for magnetite particles of different sizes. The data are also compared with the predictions of three models.

Table 4.9. Smoothed heat transfer coefficient and air holdup values for air-water-magnetite system at 308K. Column diameter: 0, 108 m, Internal: 19 mm Single tube, Particle diameters: 35.7, 49, 58, 69, 90.5, 115.5 and 137.5, Solids concentration: 0, 10, 15, 20 and 30 wt%.

Air velocity	d_p=0 w_s=0	d_p=35.7 w_s=20	d_p=49 w_s=10	d_p=58 w_s=10	d_p=58 w_s=15	d_p=69 w_s=10	d_p=69 w_s=20	d_p=69 w_s=10	d_p=90.5 w_s=20	d_p=90.5 w_s=30	d_p=115.5 w_s=10	d_p=115.5 w_s=20	d_p=115.5 w_s=30	d_p=137.5 w_s=10	d_p=137.5 w_s=20	d_p=137.5 w_s=30
Heat Transfer Coefficient																
0.015	2.96	3.00	3.30	-	-	3.50	3.30	-	-	-	-	-	-	-	-	-
0.020	3.24	3.50	3.65	-	-	3.72	3.56	-	-	-	3.70	3.80	3.75	-	-	-
0.030	3.86	3.75	3.95	-	-	4.00	4.00	-	-	-	4.32	4.35	4.25	4.25	4.30	4.40
0.040	4.28	4.20	4.25	-	-	4.20	4.25	-	-	-	4.55	4.50	4.50	4.50	4.55	4.55
0.050	4.58	4.45	4.52	-	-	4.60	4.60	-	-	-	4.70	4.70	4.75	4.75	4.75	4.80
0.060	4.72	4.63	4.72	-	-	4.75	4.75	-	-	-	4.80	4.86	5.05	4.90	4.90	5.05
0.070	4.80	4.82	4.68	-	-	4.85	4.95	-	-	-	4.93	4.95	5.11	5.10	5.05	5.15
0.080	4.92	4.97	5.00	-	-	5.00	4.98	-	-	-	5.00	5.20	5.30	5.15	5.15	5.50
0.090	5.02	5.10	5.13	-	-	5.15	5.20	-	-	-	5.15	5.35	5.35	5.20	5.55	5.55
0.100	5.12	5.20	5.32	5.90	5.75	5.40	5.55	5.65	5.68	5.90	5.40	5.50	5.65	5.45	5.70	5.75
0.150	5.50	5.80	5.75	5.95	5.98	5.65	5.72	5.82	5.96	6.07	5.75	5.60	5.80	5.80	5.75	5.85
0.200	5.68	5.94	5.93	6.10	6.18	6.00	6.05	5.97	6.15	6.30	5.80	5.90	6.10	5.90	5.90	5.90
0.250	5.76	5.95	5.95	6.15	6.25	6.00	6.05	6.15	6.27	6.38	5.95	5.95	6.15	5.95	6.15	6.15
0.300	5.78	-	-	6.35	6.38	6.00	6.03	6.35	6.40	6.45	-	-	6.15	5.95	6.20	6.20
0.333	5.77	-	-	6.33	6.30	-	-	6.32	6.45	6.45	-	-	-	-	-	-
Air Holdup																
0.015	0.030	0.027	0.030	-	-	0.030	0.032	-	-	-	-	-	-	-	-	-
0.020	0.060	0.032	0.092	-	-	0.070	0.071	-	-	-	0.045	0.030	0.028	-	-	-
0.030	0.091	0.082	0.110	-	-	0.115	0.107	-	-	-	0.055	0.050	0.051	0.053	0.051	0.055
0.040	0.129	0.120	0.128	-	-	0.130	0.125	-	-	-	0.063	0.058	0.061	0.065	0.070	0.075
0.050	0.150	0.162	0.142	-	-	0.150	0.145	-	-	-	0.110	0.105	0.103	0.091	0.090	0.100
0.060	0.180	0.166	0.165	-	-	0.190	0.161	-	-	-	0.125	0.120	0.115	0.095	0.098	0.105
0.070	0.211	0.179	0.175	-	-	0.210	0.170	-	-	-	0.145	0.133	0.120	0.130	0.120	0.117
0.080	0.220	0.191	0.186	-	-	0.207	0.180	-	-	-	0.159	0.145	0.132	0.138	0.149	0.137
0.090	0.227	0.210	0.195	-	-	0.215	0.195	-	-	-	0.176	0.158	0.135	0.165	0.160	0.160
0.100	0.226	0.222	0.221	0.210	0.203	0.225	0.205	0.228	0.185	0.165	0.190	0.167	0.144	0.195	0.190	0.180
0.150	0.247	0.235	0.247	0.227	0.225	0.240	0.226	0.245	0.222	0.207	0.218	0.220	0.195	0.232	0.225	0.224
0.200	0.270	0.271	0.280	0.250	0.247	0.246	0.245	0.270	0.265	0.247	0.238	0.255	0.242	0.270	0.259	0.260
0.250	0.293	0.277	0.295	0.290	0.286	0.278	0.280	0.310	0.295	0.275	0.276	0.305	0.285	0.294	0.294	0.290
0.300	0.324	-	-	0.330	0.310	-	-	0.344	0.330	0.305	-	-	-	0.361	0.360	0.350
0.333	0.379	-	-	0.344	0.330	-	-	0.356	0.346	0.320	-	-	-	-	-	-

particles in the powder, the three-phase system values being always smaller than the corresponding two-phase system values. The differences between the two sets of values are relatively more pronounced in the bubbling regime where coalescence is insignificant than at higher air velocities. For the air-water system, the former regime is encountered with air velocities smaller than about 0.08 ms^{-1}. In this region the differences between the two sets of values are up to about 25% for slurries of particles smaller than about 100 μm, and these increase to 40% for powders with particle sizes greater than 100 μm. For air velocities greater than 0.08 ms^{-1}, and for all the powders, the differences in the air holdup values for the two sets range between 7% and 15%.

These differences can be explained and understood on the basis of the rheology of the two- and three-phase dispersions. The presence of magnetite powder in water increases its viscosity, and this increase is greater if the weight fraction of the powder in the slurry increases. The increasing viscosity of the suspension increases the bubble size and hence the bubble velocity. The decreased residence time results in the decreased air holdup.

(b) The holdup data in Figs. 4.10A and 4.10B explicitly demonstrate the influence of slurry concentration on air holdup as the air velocity is varied over the range 0.017-0.333 ms^{-1}. In general, the holdup is nominally altered by an increase in solids in the dispersion, at least in the range 10-30 wt.%. For slurries containing particles smaller than about 100 μm, the air holdup decreases as the slurry concentration is initially increased but the slurry concentration effect becomes negligibly small as the concentration is further increased. With slurries containing particles greater than 100 μm the slurry concentration has a negligible influence on the air holdup over the entire air velocity range. It would appear that for most design purposes the influence of slurry concentration on air holdup may be neglected without any serious error.

This trend can be easily explained by the fact that bubble size depends on the magnitude of solids concentration in slurries of particles smaller than about 100 μm, and does not significantly change with concentration for slurries of particles larger than about 100 μm.

(c) The influence of particle size in the slurry on air holdup is displayed in

Fig. 4.11, where for each size in the slurry a mean set of air holdup values is considered over the entire concentration range.

On careful examination the results in Fig. 4.11 suggest a trend. The air holdup values decrease as the particle size in the slurry increases. The influence is more pronounced at lower air velocities and becomes relatively smaller at higher air velocities. At an air velocity of 0.08 ms^{-1}, the difference in the extreme values is about 12% which diminishes to about 5% at the highest air velocity. Small increments in the values of the particle diameter produce changes in the holdup values which are within the range of experimental uncertainty, and apparent trends opposite to that described may be exhibited.

In conclusion, it may be emphasized that small changes in particle size may not significantly influence the air holdup values, but relatively large changes will probably decrease the air holdup.

Experiments have been conducted for this bubble column with a seven-tube bundle to measure the air holdup at 309 K. The air holdup was measured for decreasing air velocity, with constant slumped height (1.1 m) and over a wide range of d_p and C_s. The holdup data is presented in Fig. 4.12 as a function of U_g for three different particles and two concentrations. The holdup data for the two-phase, air-water, is also shown for comparison. It is interesting to note that the holdup decreases with the increase in slurry concentration and the decrease is more for larger size particles. The experimental air holdup data is presented in Table 4.10.

4.3.7 Nitrogen - Therminol - Red Iron Oxide System

The nitrogen holdup was measured for decreasing gas velocities in the 0.108 m bubble column equipped with an internal and in slurries of red iron oxide up to 47 wt. % concentration. The internal used was either a single tube of 19, 31.8 or 50.8 mm diameter or a seven-tube bundle of 19.0 mm tubes.

The values of nitrogen holdup as a function of nitrogen velocity and slurry concentration for the four cases are shown in Fig. 4.13 and given in the Table 4.11. In each case several concentrations of the slurry are examined and nitrogen

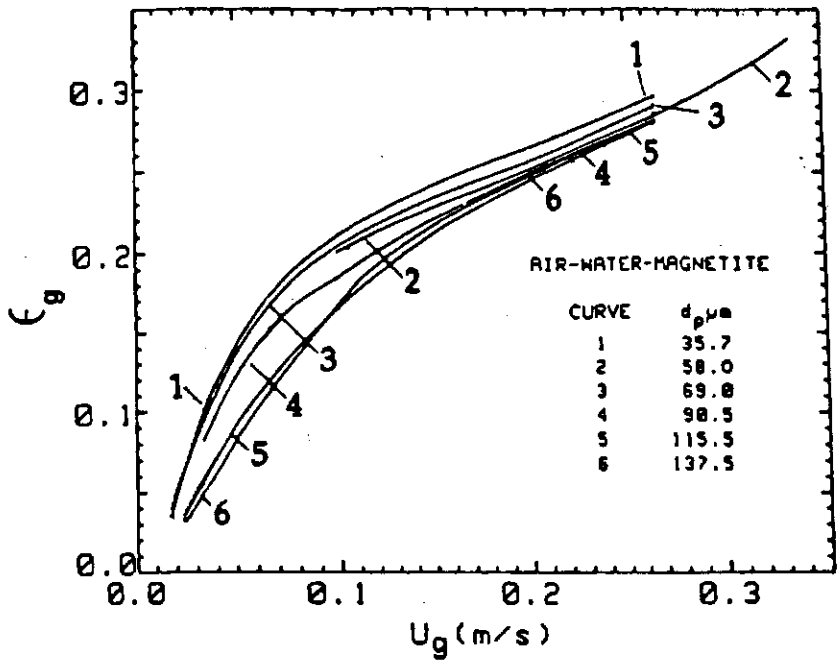

Fig. 4.11. Dependence of air holdup on particle diameter in the slurry as a function of air velocity over a slurry concentration range (10-30 wt%).

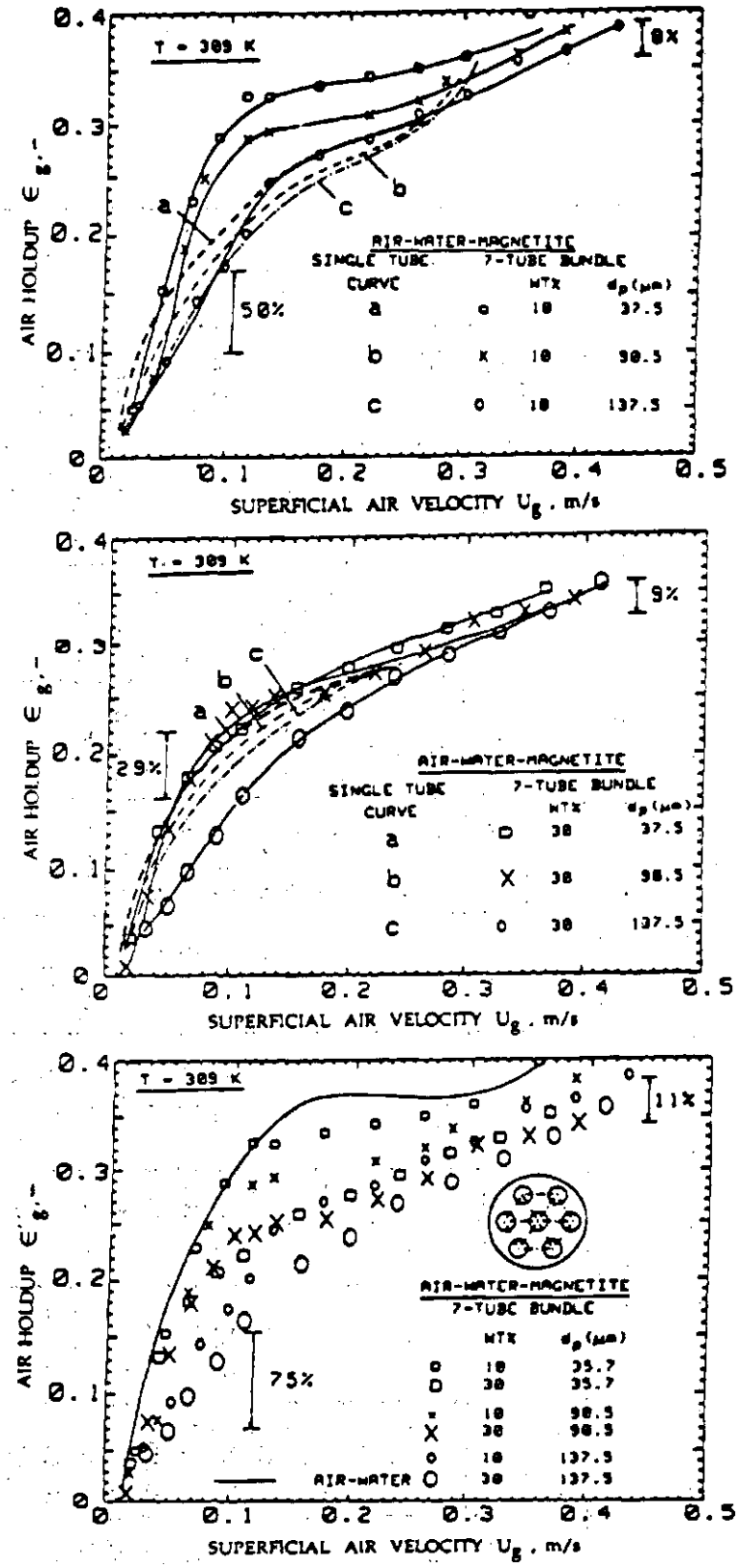

Fig. 4.12. Dependence of air holdup on air velocity, particle diameter and concentration in the slurry.

Table 4.10. Experimental air holdup values for air-water-magnetite system at 309K. Column diameter: 0.105m, Internal: Seven-tube bundle, Particle diameters: 35.7, 90.5 and 137.5μm, Solids concentrations: 10 and 30wt%.

Air Holdup											
Air-water			37.5 μm			90.0 μm			143.3 μm		
U_g(m/s)	H_e=1.1m	H_e=1.7m	U_g(m/s)	10wt%	30wt%	U_g(m/s)	10wt%	30wt%	U_g(m/s)	10wt%	30wt%
0.011	0.025	-	0.011	0.032	-	0.016	0.036	0.041	0.027	0.060	0.059
0.027	0.097	0.083	0.017	-	0.033	0.027	0.077	0.088	0.044	0.085	0.079
0.044	0.0156	0.148	0.022	0.046	-	0.038	0.091	0.147	0.071	0.151	0.110
0.061	0.214	0.195	0.044	0.149	-	0.061	0.196	0.191	0.104	0.186	0.176
0.077	0.253	0.233	0.047	-	0.037	0.075	0.256	0.224	0.128	0.252	0.221
0.110	0.316	0.301	0.061	-	0.176	0.110	0.293	0.254	0.170	0.277	0.245
0.128	0.387	0.365	0.066	0.225	-	0.128	0.299	0.263	0.213	0.292	0.260
0.170	0.388	0.372	0.088	0.284	0.209	0.170	0.310	0.280	0.256	0.317	0.288
0.213	0.361	0.348	0.104	0.303	0.218	0.213	0.316	0.284	0.280	0.334	0.310
0.256	0.357	0.350	0.110	0.323	-	0.256	0.329	0.304	0.391	0.351	0.323
0.298	0.364	0.365	0.149	0.323	0.254	0.298	0.350	0.336	0.341	0.364	0.340
0.341	0.376	0.389	0.213	0.340	0.280	0.341	0.370	0.341	0.383	0.373	0.351
0.426	0.404	0.422	0.383	0.406	0.372	-	-	-	-	-	-

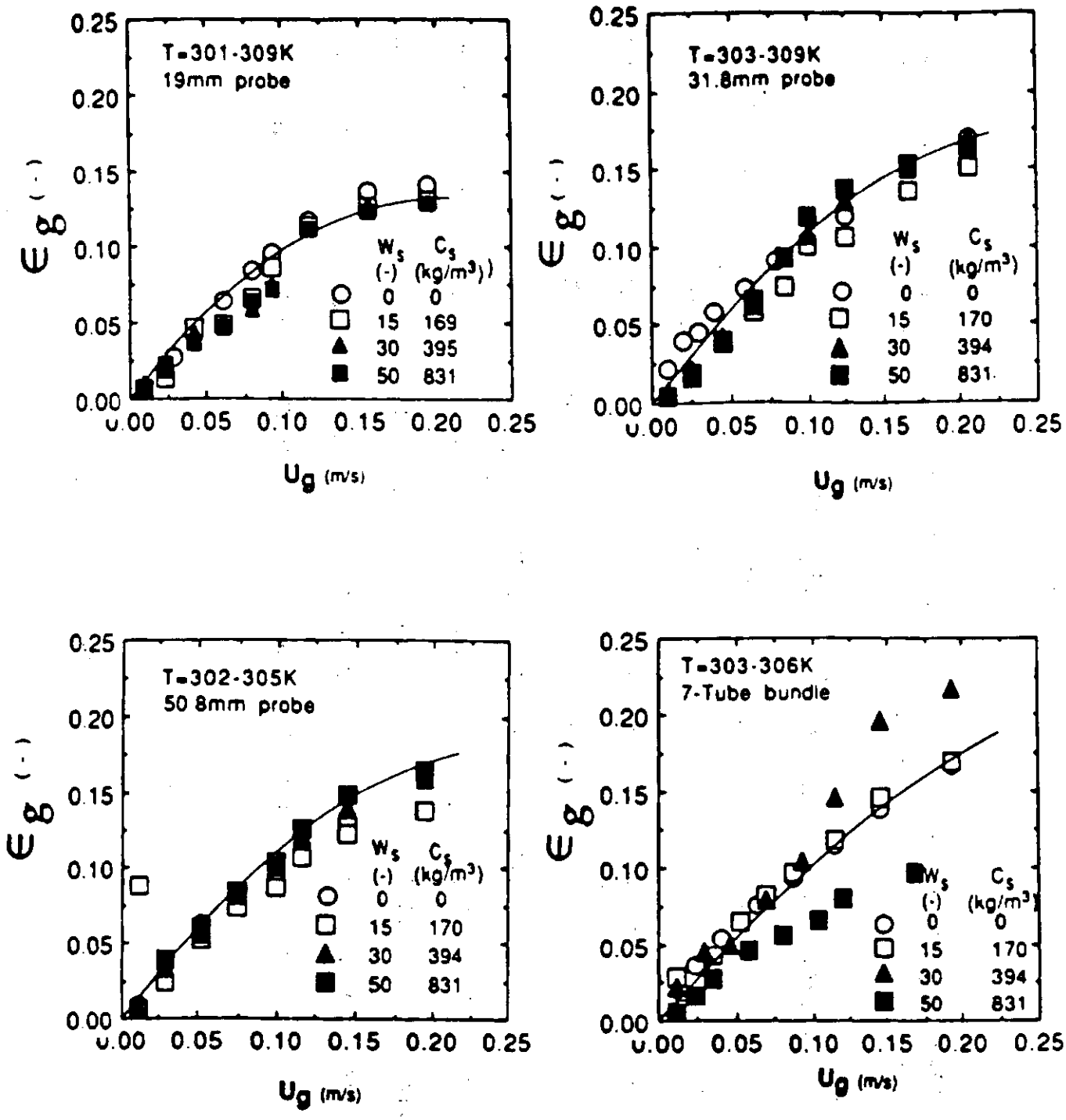

Fig. 4.13. Dependence of nitrogen holdup on nitrogen velocity and slurry concentration as determined in a bubble column equipped with heat transfer probes of different diameters and a seven-tube bundle.

Table 4.11. Smoothed nitrogen holdup values for nitrogen-Therminol-red iron oxide system at 301-309K. Column diameter: 0.108 m, Internal: 19, 31.8, 50.8 mm single tubes and seven-tube bundle. Particle diameter: 1.7 μm, Solids concentrations: 0, 15, 30 and 50 wt%.

U_g	0%	15%	30%	50%	0%	15%	30%	50%	0%	15%	30%	50%	0%	15%	30%	50%
(m/s)	19.0 mm probe				31.8 mm probe				50.8 mm probe				7 - Tube bundle			
0.025	0.021	0.020	0.020	0.020	0.041	0.028	0.020	0.018	0.025	0.023	0.028	0.030	0.040	0.045	0.038	0.022
0.050	0.054	0.045	0.041	0.040	0.067	0.052	0.048	0.042	0.051	0.048	0.054	0.058	0.065	0.072	0.062	0.040
0.075	0.083	0.070	0.059	0.057	0.089	0.071	0.082	0.070	0.076	0.070	0.080	0.086	0.090	0.089	0.098	0.055
0.100	0.104	0.092	0.087	0.082	0.105	0.090	0.100	0.102	0.096	0.086	0.103	0.110	0.108	0.120	0.120	0.168
0.125	0.119	0.110	0.109	0.108	0.122	0.110	0.125	0.122	0.118	0.105	0.124	0.130	0.127	0.138	0.172	0.080
0.150	0.130	0.123	0.122	0.121	0.140	0.122	0.142	0.146	0.136	0.120	0.140	0.148	0.142	0.153	0.195	0.090
0.175	0.138	0.131	0.129	0.127	0.150	0.138	0.158	0.152	0.150	0.134	0.155	0.162	0.157	0.170	0.210	0.098
0.200	0.143	0.135	0.132	0.130	0.162	0.150	0.161	0.160	0.162	0.142	0.170	0.175	0.170	0.182	0.220	0.106

velocity is varied from 0.01 to 0.24 m/s covering the different flow regimes, namely, discrete bubbling, bubbly churn turbulent and slugging regimes.

From Fig. 4.13, it is clear that nitrogen holdup increases steadily with increase in nitrogen velocity over the whole gas velocity range. The rate of increase of holdup with increase in gas velocity, is large in the beginning and it decreases with further increase in nitrogen velocity. A few remarks about the flow regimes, and bubbling phenomenon are essential to explain the results of Fig. 4.13. No hysteresis effect was observed for nitrogen-Therminol system in contrast with the air-water system. Also no foaming is observed for systems involving Therminol. At low nitrogen velocities ($\leq$ 3 cm/s), bubbles were formed at the distributor plate from varying regions of the plate and having an initial size of 4-5 mm in diameter. These bubbles in discrete identity rise through the liquid column and coalesce only at the top section of the liquid column (> 0.9 m) to a size as big as 15 mm in diameter. No liquid circulation is observed in the column. With further increase in nitrogen velocity bubble formation occurs over increasing portion of the distributor plate. Bubble coalescence also takes place over a larger section of the column. The coalesced bubble at a nitrogen velocity of about 8 cm/s are as large as 40 mm. The liquid circulation is observed but bubbles are not swept into these local circulating eddies to move downwards. With further increase in nitrogen gas velocity, the bubble coalescence occurs throughout the column, and the bubble size grows up to 70 mm at velocities approaching 17 cm/s. The liquid is well mixed and churned but any cellular liquid circulation pattern is not observed and bubbles always move upwards. At velocities greater than 17 cm/s, slugs are formed at the upper section of the column whose size depends upon the nature of internals.

The initial rapid increase of gas holdup for nitrogen velocities up to about 8 cm/s referred to the discrete bubbling and initial coalescing flow regimes. Here, bubbles are relatively smaller and their number increases with increase in nitrogen velocity. At nitrogen velocities greater than 8 cm/s, the bubble size increases with flow rate due to coalescence and hence the holdup increases less rapidly than for velocities smaller than 8 cm/s. For nitrogen velocities greater than 17 cm/s, the increase in holdup is very slow due to the large slugs formed in the column which move through the dispersion at a relatively much rapid

rate.

Figure 4.13 also highlights the influence of slurry concentration on nitrogen holdup. The data suggests a small dependence (± 5 percent of the mean holdup) of solids concentration on hold up. At smaller velocities (< 0.08 m/s) the holdup decreases with increase in slurry concentration while at higher velocities (> 0.08 m/s) the holdup increases with increase in slurry concentration. The experimental uncertainty also increases with increase in slurry concentration as the powder coated the column wall making it much more difficult to estimate the slurry height in the column. The variation of holdup is also dependent on the nature of internal. We estimate our experimental uncertainty to be about ± 5 percent and this is quite comparable to the variation observed in holdup values with concentration. We, therefore, conclude that for such small size powders (micron size range), the influence of changes in slurry concentration on holdup is small and can be neglected in most design studies. Table 4.11 lists the smoothed experimental holdup values for different configurations as a function of slurry concentration and nitrogen velocity.

To highlight the dependence of nitrogen holdup on the size and configuration of internals, the experimental data are displayed in Fig. 4.14. Figure 4.14 presents the data for nitrogen-Therminol for the four internals. The holdup values for the tube bundle and the two larger probes are about the same while for the smallest internal the corresponding values are smaller. The addition of solids in general has negligible influence on holdup. Pronounced bubble coalescence was observed and slugs formed in the upper region of the column. This resulted in lower gas holdup.

4.3.8 Nitrogen - Therminol - Magnetite System

Nitrogen gas holdup measurements were taken with three single tubes and a seven-tube bundle for decreasing nitrogen velocity in the batch mode. Three different particles of magnetite (27.7, 36.6 and 46.0 μm) are used in the slurry concentration range up to 50% weight precent.

In Fig. 4.15 are presented the nitrogen holdup data as a function of nitrogen

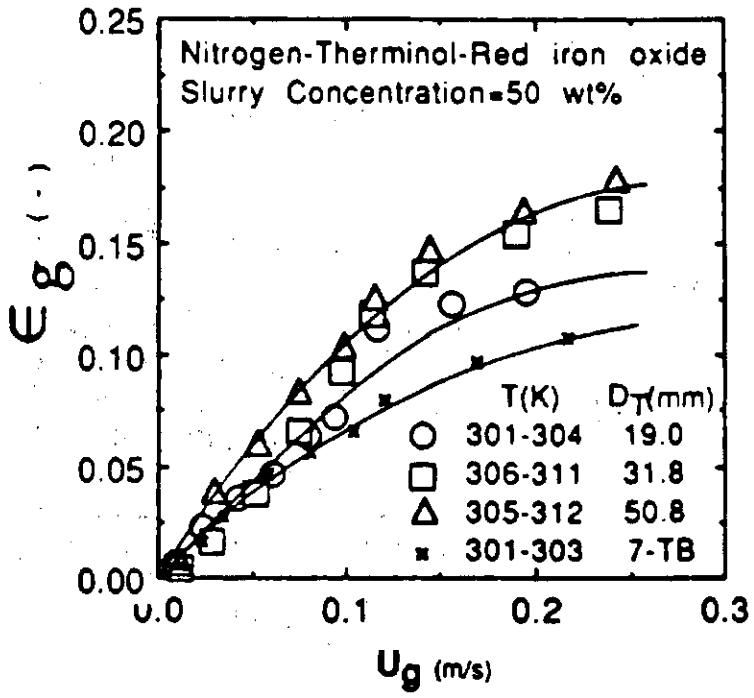

Fig. 4.14. Variation of holdup for nitrogen-Therminol-red iron oxide system for different internals and nitrogen velocity.

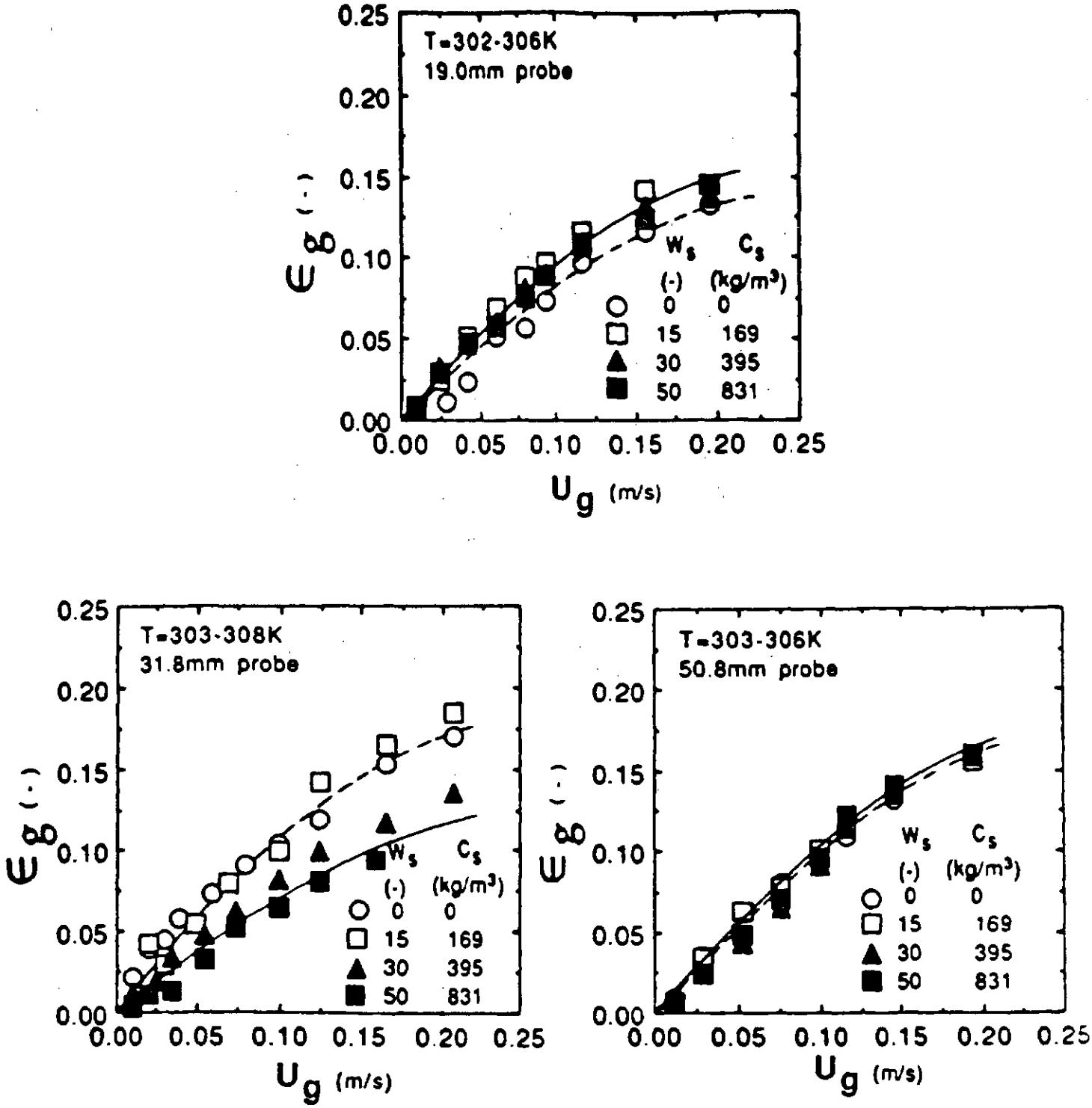

Fig. 4.15. Influence of nitrogen velocity and solids concentration on nitrogen holdup for the nitrogen-Therminol-magnetite (36.6 μm) system for the three probes. - - - 0, —— 50, weight percent smooth plots.